International Journal of Bioprinting

RESEARCH ARTICLE

Using 3D-bioprinted models to study pediatric neural crest-derived tumors

Colin H. Quinn[1†], Andee M. Beierle[2†], Janet R. Julson[1], Michael E. Erwin[1], Hasan Alrefai[2], Hooper R. Markert[1], Jerry E. Stewart[1], Sara Claire Hutchins[3], Laura V. Bownes[1], Jamie M. Aye[3], Elizabeth Mroczek-Musulman[4], Patricia H. Hicks[4], Karina J. Yoon[5], Christopher D. Willey[2]*, Elizabeth A. Beierle[1]*

[1]Division of Pediatric Surgery, Department of Surgery, University of Alabama, Birmingham, Birmingham, AL, 35205, USA

[2]Department of Radiation Oncology, University of Alabama at Birmingham, Birmingham, AL, 35205, USA

[3]Division of Pediatric Hematology Oncology, Department of Pediatrics, University of Alabama at Birmingham, Birmingham, AL, 35233, USA

[4]Department of Pathology, University of Alabama at Birmingham, Birmingham, AL, 35233, USA

[5]Department of Pharmacology and Toxicology, University of Alabama at Birmingham, Birmingham, AL, 35294, USA

(This article belongs to the *Special Issue: Bioprinting process for tumor model development*)

Abstract

The use of three-dimensional (3D) bioprinting has remained at the forefront of tissue engineering and has recently been employed for generating bioprinted solid tumors to be used as cancer models to test therapeutics. In pediatrics, neural crest-derived tumors are the most common type of extracranial solid tumors. There are only a few tumor-specific therapies that directly target these tumors, and the lack of new therapies remains detrimental to improving the outcomes for these patients. The absence of more efficacious therapies for pediatric solid tumors, in general, may be due to the inability of the currently employed preclinical models to recapitulate the solid tumor phenotype. In this study, we utilized 3D bioprinting to generate neural crest-derived solid tumors. The bioprinted tumors consisted of cells from established cell lines and patient-derived xenograft tumors mixed with a 6% gelatin/1% sodium alginate bioink. The viability and morphology of the bioprints were analyzed via bioluminescence and immunohisto chemistry, respectively. We compared the bioprints to traditional two-dimensional (2D) cell culture under conditions such as hypoxia and therapeutics. We successfully produced viable neural crest-derived tumors that retained the histology and immunostaining characteristics of the original parent tumors. The bioprinted tumors propagated in culture and grew in orthotopic murine models. Furthermore, compared to cells grown in traditional 2D culture, the bioprinted tumors were resistant to hypoxia and chemotherapeutics, suggesting that the bioprints exhibited a phenotype that is consistent with that seen clinically in solid tumors, thus potentially making this model superior to traditional 2D culture for preclinical investigations. Future applications of this technology entail the potential to rapidly print pediatric solid tumors for use in high-throughput drug studies, expediting the identification of novel, individualized therapies.

Keywords: 3D bioprinting; Neuroblastoma; Neuroendocrine; Pediatrics; Targeted therapy; Patient-derived xenografts

[†]These authors contributed equally to this work.

***Corresponding authors:**
Christopher D. Willey (cwilley@uabmc.edu)

Elizabeth A. Beierle (elizabeth.beierle@childrensal.org)

Citation: Quinn CH, Beierle AM, Julson JR, *et al*., 2023, Using 3D-bioprinted models to study pediatric neural crest-derived tumors. *Int J Bioprint*. https://doi.org/10.18063/ijb.723

Received: December 17, 2022
Accepted: February 21, 2023
Published Online: March 29, 2023

1. Introduction

The outcomes for children with hematologic malignancies have substantially improved in the last 30 years, but the same success is not evident in children with solid tumors[1]. Tumors of neural crest origin, including neuroblastoma, melanoma, peripheral malignant nerve sheath tumor, and gastroenteropancreatic neuroendocrine tumors (NETs), continue to have dismal prognoses. In the pediatric population, neuroblastoma is the most common neural crest-derived tumor, and children with high-risk disease have less than a 50% chance of a 5-year event-free survival[2]. Pediatric NETs, which are the rarest, may have survival rates as low as 10%[3]. Therefore, discovering therapies to improve outcomes in these diseases remains a necessary endeavor.

Solid tumor modeling has traditionally relied on two-dimensional (2D) cell culture. However, this method cannot recapitulate the complexities of solid tumors, including tumor cell heterogeneity and tumor microenvironment. Animal models have also been employed, but they are time-consuming, thus further delaying the clinical translation of experimental treatments. Tumor organoids are another cell culture approach, in which these organoid models rely on tumor cells or tumor stem cells to create their three-dimensional (3D) structure[4]. All of these approaches fall short of 3D bioprinting. 3D bioprinting cancer cells into microtumors allows for the generation of specific tumor architecture with multiple cell types and provides the opportunity for scalability and more manipulation[5,6]. Investigators have used 3D bioprinting for adult tumor types, including breast and pancreatic cancers as well as brain tumors, using established cancer cell lines and patient-derived tumors[7,8]. These 3D-printed microtumors demonstrated the tumor phenotype and recapitulated the tumor microenvironment.

For the current study, we aimed to create 3D-bioprinted tumors of pediatric neural crest-derived tumors using established cell lines and patient-derived xenograft (PDX) cells. We hypothesized that these 3D bioprint models would provide an improved representation of the solid tumor phenotype compared to the traditional 2D culture method. Using a combination of approaches, we produced tumor models with properties consistent with the solid tumors of origin. Additionally, we were able to scale this 3D model for high-throughput drug screening, which could be applied to personalized cancer therapy testing.

2. Materials and methods

2.1. Cell lines

Both long-term passage and patient-derived xenograft (PDX) lines were used in this study. Both cell lines were of human origin and annually validated via short tandem repeats as recommended by the American Type Culture Collection (ATCC, Manassas, VA, USA). PDX tumors were also validated via histology. SK-N-AS (*MYCN*-non-amplified, CRL-2137) and SK-N-BE(2) (*MYCN*-amplified, CRL-2271), were purchased from ATCC. SK-N-AS cells were cultured and tested in Dulbecco's Modified Eagle's Medium (DMEM; 30-2601, ATCC) containing 10% fetal bovine serum (FBS; HyClone, South Logan, UT, USA), 4 mmol/L L-glutamine (Thermo Fisher Scientific Inc., Waltham, MA, USA), 1 μmol/L nonessential amino acids, and 1 μg/mL penicillin/streptomycin (Sigma Aldrich, Burlington, MA, USA). SK-N-BE(2) cells were cultured and tested in a 1:1 mixture of minimum Eagle's medium and Ham's F-12 medium (30-2004, ATCC) with 10% FBS (HyClone), 2 mmol/L L-glutamine (Thermo Fisher Scientific Inc.), 1 μmol/L nonessential amino acids, and 1 μg/mL penicillin/streptomycin (Sigma Aldrich).

Two human neuroblastoma PDXs, COA3 and COA6, and a gastroenteropancreatic human NETPDX, COA109, were established and fully characterized as described in previous publications[9,10]. The PDXs were passed through animals as these cells cannot be propagated in traditional 2D cell culture. For experimentation, dissociated PDX tumor cells were maintained and tested in neurobasal medium (NB) (Life Technologies, Thermo Fisher Scientific, Waltham, MA)supplemented with B-27 without vitamin A (Life Technologies), N2 (Life Technologies), amphotericin B (250 μg/mL, HyClone), gentamicin (50 μg/mL, Millipore), L-glutamine (2 mM, Thermo Fisher Scientific Inc.), epidermal growth factor (EGF; 10 ng/mL, Miltenyi Biotec, San Diego, CA, USA), and fibroblast growth factor (FGF; 10 ng/mL, Miltenyi Biotec).

2.2. Patient-derived xenografts (PDXs)

The PDXs used in this study included two high-risk neuroblastomas (COA3 and COA6) and one pediatric, high-grade neuroendocrine-like tumor (COA109) that were derived from tumor samples of patients at Children's Hospital of Alabama[10,11]. The tumors were obtained as previously described[10] under the University of Alabama at Birmingham (UAB) Institutional Review Board (IRB)-approved protocol (IRB 130627006) and in accordance with the Declaration of Helsinki and the guidelines of the National Institutes of Health. Following written informed consent from parents or guardians and written informed assent from the patients as necessary, fresh tumor samples were acquired and partitioned for (i) storage at −80°C; (ii) paraffin embedding; and (iii) implantation into the flanks of athymic nude mice in a mixture of 25% Matrigel (Corning Inc., Corning, NY, USA) and Roswell Park Memorial Institute (RPMI) 1640 (30-2001, ATCC) following UAB Institutional Animal Care and

Use Committee (IACUC) protocol (IACUC-09186) for PDX maintenance. Once the PDX tumors reached the size dictated by IACUC parameters, they were dissociated into a single cell suspension via the Mouse Tumor Dissociation Kit (Miltenyi Biotec, Bergisch Gladbach, Germany) following the manufacturer's protocol and utilized for *in vitro* studies.

2.3. 3D bioprinting

Two different bioprinting methods were employed for this study. The initial bioprinting method involved layered bioprinting, consisting of (i) a bottom layer of bioink composed of 1% sodium alginate and 6% gelatin (Pronova UP-LVM, Dupont Nutrition Norge As, Sandvika, Norway); (ii) a middle layer of cells (5×10^5 cells in 15 µL); and (iii) a top layer of bioink printed in the same wayas the bottom layer into 12-well plates. In order to create the first layer, the bioink was loaded into a 3 mL printing cartridge (Cellink, Boston, MA, USA) and placed into a 3 mL pneumatic printheadin Cellink's BIO X printer. The bioink was then extruded as a droplet into the plate through Cellink's 20-gauge 1/2 inch blunt tip needle at a pressure of 10 kPa for 0.3 s to create a droplet volume of 100 µL. Cells (15 µL) were then pipetted onto this bottom layer. Next, a second layer of bioink was printed onto this structure following the previously used pressure and extrusion time. Diluted calcium chloride (100 µL, C1016-500G, Sigma-Aldrich) to 2% in distilled water was then added on to the bioprint for 20 min to achieve crosslinking. The prints were then washed with 500 µL of sterile phosphate-buffered saline (PBS), and all the liquid was removed from the well containing the bioprint. Finally, 2 mL of the cell line's respective media was placed in the well. The prints were used 24 h later for experimentation.

The second method employed for bioprinting involved mixing the tumor cells directly into the bioink to create a homogeneous bioink solution. A bioink (1,000 µL) composed of 1% sodium alginate and 6% gelatin was prepared and loaded into a BD Plastipak 3 mL syringe with Luer-Lok tip (Fischer Scientific). A female-female Luer-Lok connector (IMI, Pompano Beach, FL, USA) was then connected to the end of the 3 mL syringe. Tumor cells were prepared in a volume of 100 µL such that the final cell density in the bioink solution would be 10^7 cells per 100 µL of bioink. In order to accomplish the mixing, the prepared tumor cells were placed into a separate 3 mL syringe with Luer-Lok tip and connected to the free end of the Luer-Lok connector. The bioink and cells were then interspersed with one another, creating a homogeneous mixture by repeatedly pushing the materials back and forth across the connector. The cell–bioink mixture was then loaded into a 3 mL printing cartridge and placed into a 3 mL pneumatic print head in Cellink's BIO X printer. The bioink was then extruded as a droplet through Cellink's 22-gauge 1/2inch blunt tip needle at a pressure of 10 kPa for 1.2 s to create a droplet volume of 30 µL onto a 3 µM pore transwell insert (Corning Life Sciences, Tewksbury, MA, USA) in a 24-well plate. Then, 100 µL of 2% calcium chloride was added onto the bioprinted structures for 5 min to achieve crosslinking. The prints were then washed with 500 µL of sterile PBS, and all the liquid was removed from the transwell containing the bioprint. Finally, 2 mL of the cell line's respective media was placed in the well. The prints were incubated at 37°C in 5% carbon dioxide (CO_2) for 5 days to form tumors, and the media were replaced daily.

In order to test the bioprints in a high-throughput nature, the bioprints created using the mixed method were scaled down to a 96-well plate. The preparation of the cell-bioink solution followed the same procedure listed above for the mixed method, and the final cell density in the bioink solution (10^7 cells per 100 µL of bioink) was the same. The bioink was extruded as a droplet through Cellink's 22-gauge 1/2 inch blunt tip needle at a pressure of 10 kPa for 0.4 s to create a droplet volume of 10 µL into a 96-well plate. Calcium chloride (2%, 40 µL) was added onto the bioprinted structures for 5 min to achieve crosslinking. The prints were then washed with 100 µL of sterile PBS, and all the liquid was removed from the transwell containing the bioprint. Finally, 200 µL of the cell line's respective media was placed in the well. The prints were used 24 h later for experimentation.

Many aspects of the bioprinting protocol were adapted from the established bioprinting protocol from Cellink (https://www.cellink.com/wp-content/uploads/2019/03/Bioprinting-Protocol-CELLINK-Bioink_14-Jun-2021.pdf), including, but not limited to, the ratio of the bioink to cells, the technique for mixing the cells with the bioink, the printing pressures utilized, the needle size, and the process for crosslinking with calcium chloride (**Supplementary File**, **Table S1**). The decision to use the bioink composed of 1% sodium alginate and 6% gelatin (Pronova UP-LVM, Dupont Nutrition Norge As, Sandvika, Norway) and for the cell density within the bioprints was supported by the successful bioprints created by Langer *et al.*[8].

The utilization of 3D bioprinters allows for consistency and accuracy in the creation of 3D tumor models. Cellink's BIO X bioprinter has a calibration system that allows for its bioprints to be placed with precision in the desired location. The methods described in this paper utilized the droplet feature of the printer, which allows bioink droplets to be extruded from the bioprinter and does not require a specified pattern to be programmed into the printer. In the present study, the bioprints were created using the droplet approach in view of its simplicity, especially as it applies to creating and testing bioprints with a high-throughput

approach. CellTiter Glo Luminescent Cell Viability Assay (Promega, Madison, WI, USA)was performed to ensure that the selected printing pressure did not negatively impact the viability of cells (**Supplementary File**, **Figure S1**).

2.4. Reagents

CalceinAM (C1430),a cell-permeant dye used to stain live tumor cells, and SYTOX Orange nucleic acid stain (S11368) used to stain dead tumor cells were purchased from Thermo Fischer Scientific. The antibodies used included rabbit antichromogranin A (ab15160) from Abcam (Cambridge, MA, USA) and rabbit antineuron-specific enolase (NSE) (AB951-I).Anti-rabbit immunoglobulin (Ig)G (NI0-1) was purchased from Millipore Sigma. Cisplatin was obtained from Cayman Chemical Company (13119, Ann Arbor, MI, USA), and trametinib, a small molecule inhibitor of MEK1/2, was purchased from Selleckchem (Houston, TX, USA).

2.5. Immunohistochemistry (IHC)

In vivo tumor samples were formalin-fixed, paraffin-embedded, cut into 4 μm sections, and processed as previously described[12]. The 3D-bioprinted tumors were immediately fixed in 80% ethanol for at least 24 h following experimentation. The fixed bioprinted tumors were then processed and embedded as noted for *in vivo* tumors. For both *in vivo* and 3D-bioprinted tumors, standard hematoxylin and eosin (H&E) staining methods were utilized. Chromogranin A (1:100) and NSE (1:25) staining was performed by adding primary antibody to slides for overnight incubation in a humidity chamber at 4°C. The slides were washed with PBS, and rabbit secondary antibody (R.T.U. biotinylated universal antibody, Vector Laboratories, Burlingame, CA, USA) was added for 30 min at 22°C. The reaction was completed with VECTASTAIN Elite ABC reagent (PK-7100, Vector Laboratories) at room temperature for 30 min, and Metal-Enhanced DAB Substrate (Thermo Fisher Scientific) was applied for 2 min. All slides with primary antibody were counterstained with hematoxylin and had negative controls stained with anti-IgG at 1 μg/mL.

2.6. Viability studies

The viability of homogenous mixed 3D-bioprinted tumors (24-well plates) was assessed via Calcein AM staining and ImageJ analysis (Version 1.49, http://imagej.nih.gov/ij, accessed on July 17, 2022) as described in a previous publication[13]. The viability of the 96-well plate mixed tumors was determined with alamarBlue colorimetric assays (Thermo Fisher Scientific). In 96-well plates, 3D-bioprinted tumors were printed as described and treated with cisplatin or trametinib and an equivalent concentration of vehicle (dimethyl sulfoxide, DMSO), as a control, at increasing concentrations. After 24 h, alamarBlue dye (10 μL, Thermo Fisher Scientific) was added, and absorbance was measured using a microplate reader (Epoch Microplate Spectrophotometer, BioTek Instruments, Winooski, VT, USA) at 570 nm and 600 nm. The viability of 2D-cultured cells was also assessed with alamarBlue,and the cells (1.5×10^5) were plated in 96-well plates and treated with the same conditions. The viability of cells from at least three biologic replicates was reported as fold change ± standard error of the mean (SEM).

2.7. *In vivo* studies

SK-N-AS and COA109 cells were used to print mixed 3D bioprints. The resulting bioprints were then minced and combined with 25% Matrigel/RPMI for injection into the right flank of athymic nude mice. This study was conducted under UAB IACUC approval (IACUC-09064) and in accordance with national, international, and NIH guidelines. The animals were maintained in pathogen free environment with free access to food and water. The tumor size was measured once a week, while the overall body condition was monitored daily. Per the National Cancer Institute's guidelines, the formula (width^2 × length)/2 was used to calculate tumor volume, with width being the smaller value[14].The animals were humanely euthanized and tumors were harvested once IACUC parameters were met. The tumor specimens were divided for storage at −80°C and paraffin-embedded for IHC studies.

2.8. *Ex vivo* studies

SK-N-AS cells were printed as layered 3D bioprints on the upper rowof a 12-well plate, while additional SK-N-AS cells were cultured under 2D conditions at the lower row(5×10^5 in 2 mL of media). The bioprints and cultured cells were preliminarily incubated overnight under normoxic conditions at 37°C in 5% CO_2 and then transferred to a hypoxia chamber at 1% oxygen (O_2) for 120 h. The media were replaced at the midpoint of the experiment.

After 120 h, the tumors were stained with Calcein AM for viable cells and counterstained with SYTOX Orange for dead tumor cells at 1:1000 for 30 min. Following staining, a minimum of nine images were taken using EVOS (AMG EVOS FL Digital Inverted Imaging System) at 10× magnification. The images were then individually analyzed with ImageJ software (Version 1.49, http://imagej.nih.gov/ij, accessed on September 10, 2022), where the total fluorescence area positive for Calcein AM was compared to the total fluorescence area positive for SYTOX Orange to determine the tumor viability. In order to determine the viability of 2D-cultured tumor cells under hypoxic conditions, the surrounding media were collected, and 0.5 mL of Trypsin-EDTA (0.05%, with phenol red; Thermo Fisher Scientific) was added to detach cells from the well plate. The detached cells were then pelleted, resuspended

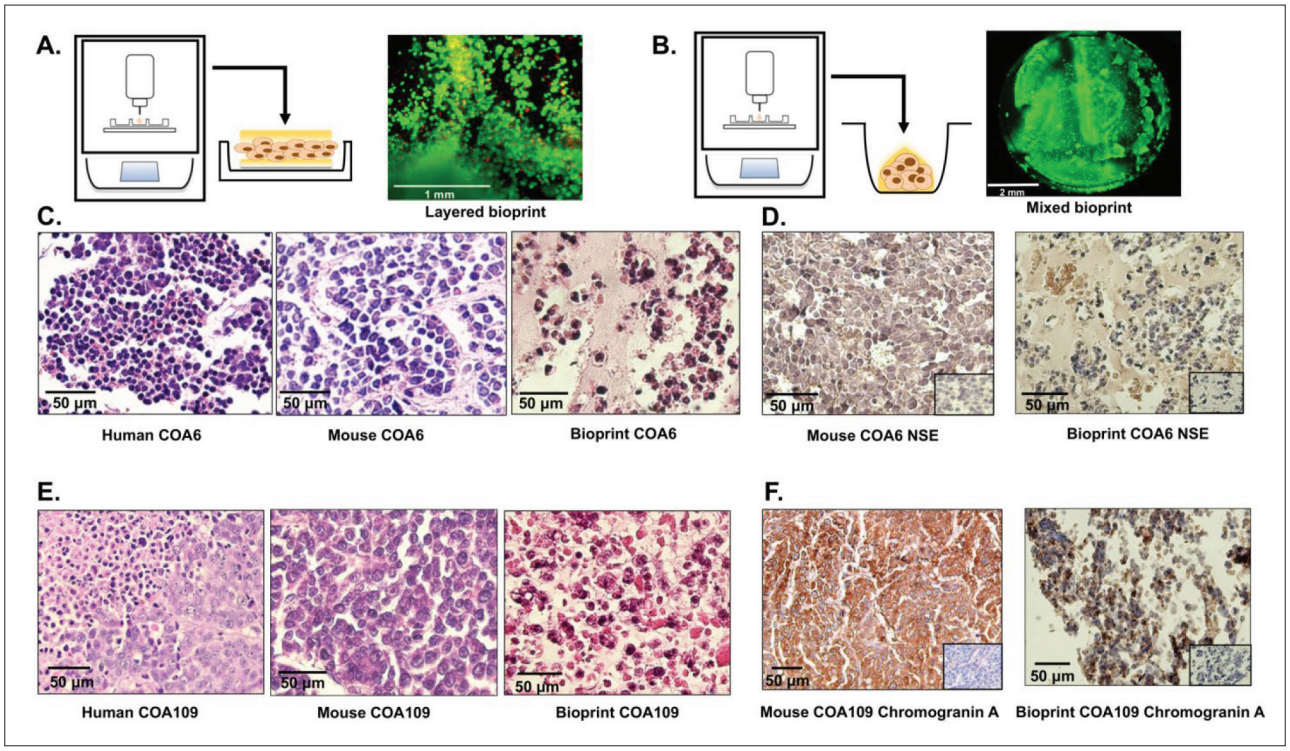

Figure 1. Three-dimensional (3D) bioprinting model of pediatric neural crest tumors. (A) Cellink's 3D printer was utilized to produce bioprinted tumors. The first model was a layered bioprint. Cancer cells (5×10^5 cells per print) were placed between two layers of 1% sodium alginate and 6% gelatin bioink, which was then crosslinked with calcium chloride for support. Calcein AM (green) and SYTOX Orange (red) wereused to identify viable and dead tumor cells, respectively, in the layered bioprint. (B) The second model was a mixed bioprint. Tumor cells (10^7 cells per print) were mixed with the 1% sodium alginate and 6% gelatin bioink and printed as a homogenous mixture, which was then crosslinked with calcium chloride. Calcein AM (green) stained viable tumor cells in the mixed bioprint. (C) Hematoxylin and eosin (H&E) staining was performed on COA6 bioprinted tumors and demonstrated that the bioprinted tumor (right panel) had similar morphology to the original tumor (left panel) and human PDX tumor from mouse (middle panel). (D) Immunostaining for neuron specific enolase (NSE), which is normally positive in neuroblastoma, was positive in the COA6 bioprinted tumor (right panel) and human PDX tumor from mouse (left panel). (E) H&E staining was performed on COA109 bioprinted tumors and demonstrated that the bioprinted tumor (right panel) hadsimilar morphology to the original tumor (left panel) and human PDX tumor from mouse (middle image). (F) Immunostaining for chromogranin A was completed on the COA109 bioprinted tumor and compared to the COA109 PDX from mouse. Chromogranin A staining was similar between the bioprint (right panel)and the murine PDX tumor (left panel). Negative control staining with IgG was performed for each run of immunostaining and is represented by the insets in the lower right corner of the photomicrographs.

in the collected media, stained with trypan blue (Gibco), and counted for alive and dead cells.

2.9. High-throughput model

SK-N-AS, COA6, and COA109 cells were used to print mixed 3D bioprints onto 96-well plates. Following a 24-h incubation, these 3D-bioprinted tumors were treated with cisplatin (SK-N-AS and COA6, 0–25 µM) or trametinib (COA109, 0–25 nM) and an equivalent concentration of vehicle (DMSO), as control. Refer to subsection **2.6.** for further details of the procedure.

2.10. Data analysis

Each experiment was completed with at least three biological replicates unless indicated, anddata were reported as mean ± SEM. Statistical analysis was performed with GraphPad Prism 9.0 using Student's t-test, analysis of variance (ANOVA), or chi-squaredtest as appropriate,with $P < 0.05$ considered significant.

3. Results

3.1. Tumor morphology is replicated in bioprinted models

We aimed to create a preclinical model using 3D bioprinting to generate tumors from established long-term passaged cell lines and PDXs. We designed two types of bioprints: a layered print with cancer cells between two layers of bioink (Figure 1A), and a mixed print comprising a homogenous mixture of cancer cells and bioink (Figure 1B). The bioprints were stained with Calcein AM to detect alive cells. Both layered (Figure 1A, right panel) and mixed (Figure 1B, right panel) prints demonstrated green fluorescence, indicating that both bioprinting methods

produced viable tumors. The printed bioink without cancer cells was plated in media withCalcein AM,and images were taken without(**Supplementary File**, **Figure S2A**) and withfluorescence (**Supplementary File**, **Figure S2B**) using a FITC laser. No fluorescence was detected under either condition, indicating that the fluorescence detected in the 3D-bioprinted tumors represented live tumor cells, not autofluorescence of the bioink.

In order to determine if the bioprinted models were representative of the tumors from the patients or those propagated in animals, IHC studies were performed. H&E staining of the bioprints demonstrated a similar morphology with that observed in the original tumor and PDX from mouse (Figure 1C and E) for both COA6 and COA109. Specifically, the COA6 bioprint tumor retained features of small round blue cells, while the COA109 bioprint demonstrated "salt and pepper" appearance (Figure 1E, right panel), which are typical of neuroendocrine tumors[15]. Next, we performed immunostaining for commonly utilized tumor markers, including NSE for neuroblastoma and chromogranin A for neuroendocrine tumors. The human neuroblastoma COA6 bioprint stained positive for NSE (Figure 1D, right panel), while the human neuroendocrine COA109 bioprint stained positive for chromogranin A (Figure 1F, right panel), indicating that the bioprints retained NET and neuroblastoma protein markers.

3.2. *In vivo* growth of bioprinted models

In order to evaluate the tumorigenicity of the bioprints, we used the mixed bioprint method and a murine flank model. We first printed SK-N-AS cells with the mixed model (Figure 2A). After growing in culture for 5 days, the SK-N-AS bioprinted microtumor was minced and implanted into the flank of a nude mouse (Figure 2A). The growth was consistent with other SK-N-AS orthotopic tumors grown in mice[16]. Once the implanted microtumor reached 2,000 mm^3, it was harvested for IHC studies. H&E staining showed that the tumor growing in the mouse, from the bioprinted microtumor, retained SK-N-AS morphology (Figure 2B, middle panel) as compared to SK-N-AS flank tumors(Figure 2B, left panel) and stained positive for NSE (Figure 2B, right panel), indicating that the bioprint tumor was a neuroblastoma. We repeated a similar experiment using the COA109 PDX (Figure 2C). There were no notable differences on H&E between the COA109 propagated through a mouse (Figure 1E, middle panel) or the COA109 bioprinted microtumor grown in the animal (Figure 2D, left panel). The neuroendocrine features were retained in the printed microtumor as demonstrated by positive chromogranin staining (Figure 2D, right panel).

3.3. Bioprinted tumors are resistant to hypoxia

Solid tumors, such as neuroblastoma, grow under hypoxic conditions *in vivo*[17,18]. We aimed to compare the ability of 3D-bioprinted tumors to 2D-cultured cells to survive hypoxic conditions. SK-N-AS cells were printed as layered bioprinted tumors (Figure 1A, left panel) and compared to 2D-cultured SK-N-AS cells. The cells and bioprinted models were exposed to 1% $O_2$for 5 days. In order to count the number of alive versus dead cells due to hypoxia, fluorescence staining was used to evaluate viability of the bioprints, while trypan blue stain was used to assess the viability of 2D-cultured cells. The percentage of viable cells in the bioprinted tumors grown in hypoxia was significantly higher than that observed in cells grown in hypoxic 2D culture. The bioprinted tumors had an average of 69 ± 9% viability compared to cells in the 2D culture, with 33 ± 7% viability (Figure 3A). A representative image of a bioprinted tumor shows areas of tumor cell death (Figure 3B, red fluorescence) surrounded by alive tumor cells (Figure 3B, green fluorescence).

3.4. Mixed bioprinted models for *ex vivo* studies

PDXs can better recapitulate human conditions than established, long-term passaged cell lines; however, it remains a challenge to perform *in vivo* studies with PDXs due to their slow and inconsistent growth rates[19]. We hypothesized that bioprinted PDX models could be employed to test potential therapeutics in an *ex vivo* fashion. Both COA6 and COA109 bioprinted tumors were produced using the mixed bioprinting method (Figure 1A, left panel) and allowed to grow for 5 days. Chemotherapeutic agents including cisplatin (10 μM), which is commonly employed for neuroblastoma, and trametinib (100 nM), a MEK1/2 inhibitor used to treat NETs, were added to the media of COA6 or COA109 bioprints, respectively. After 10 days, Calcein AM was used to detect viable cells. Viability was quantitated by calculating the mean integrated density (MID) of the fluorescence of each bioprint, as these mixed bioprinted tumors were larger than the layered bioprinted tumors and required the inclusion of intensity in determining viability (Figure 4A). Compared to those treated with vehicle, COA6 bioprinted tumors treated with cisplatin showed a significant decrease in MID (1713 ± 268 pixels/mm^2 versus 4878 ± 306 pixels/mm^2, cisplatin versus vehicle, $P \leq 0.0001$, Figure 4A and B). Compared to bioprinted tumors treated with vehicle, COA109 bioprinted tumors treated with trametinib had significantly less MID, indicating fewer viable cells (1442 ± 172 pixels/mm^2 versus 2336 ± 120 pixels/mm^2, trametinib versus vehicle, $P \leq 0.001$, Figure 4D and E). These results demonstrate that 3D-bioprinted models may be used to test PDX cells *ex vivo*.

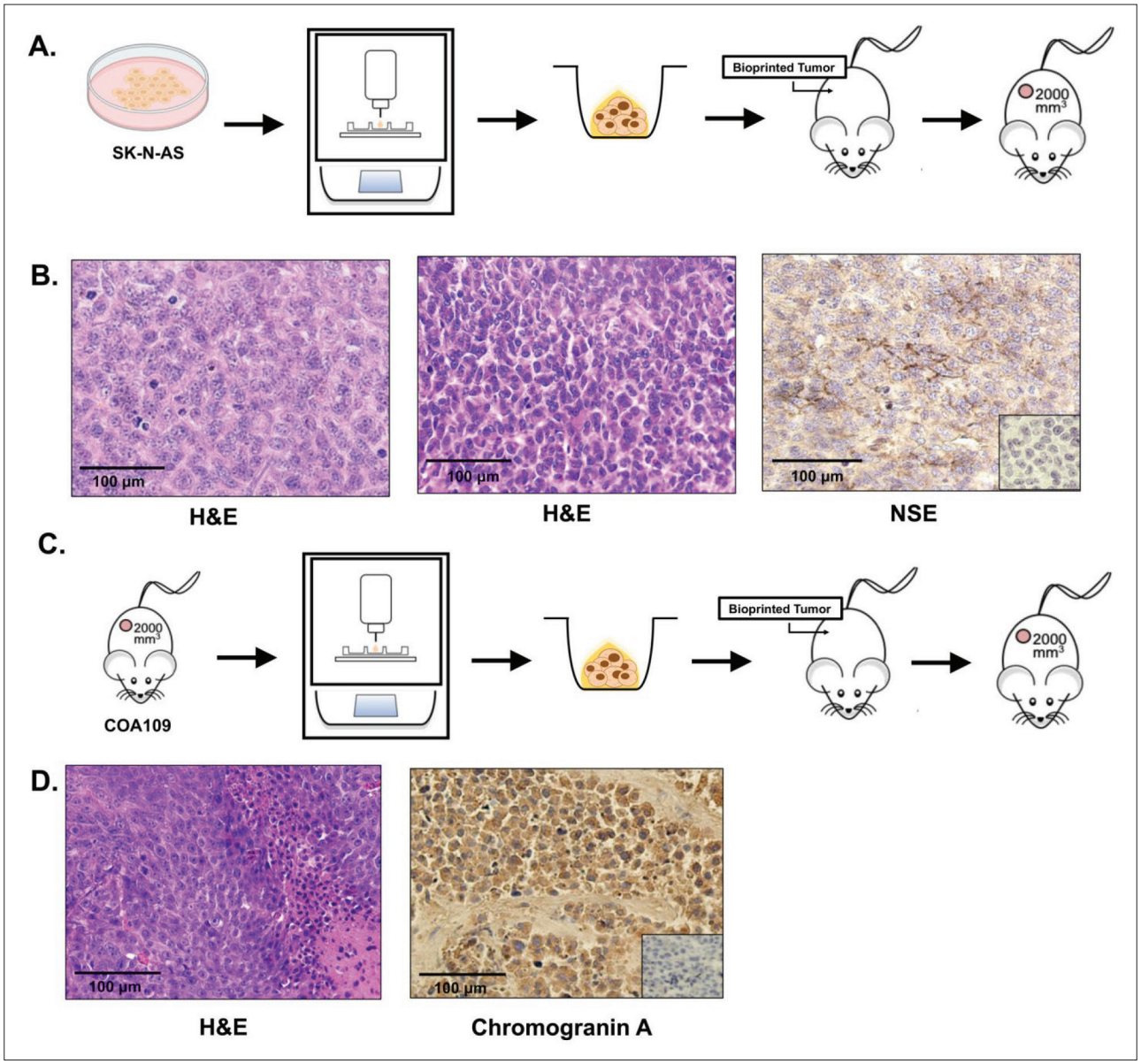

Figure 2. Bioprinted models propagate *in vivo*. (A)SK-N-AS cells were printed using the mixed bioprinting method, and the bioprints were grown in culture for 5 days. The resulting bioprinted tumor was minced and implanted into the subcutaneous space of the flank of an athymic nude mouse. (B) The flank tumors from the bioprinted models were compared to SK-N-AS flank tumors grown from 2D-cultured cells. Hematoxylin and eosin (H&E) staining demonstrated that the tumors from the 3D-bioprinted cells (right panel)had the same morphology as thatin SK-N-AS flank tumors grown from 2D-cultured cells (left panel). Immunostaining of the tumors from implanted 3D-bioprinted cells was positive for NSE staining, indicating that the 3D-bioprinted cellsretained the immunostaining properties consistent with neuroblastoma. (C) A COA109 patient-derived xenograft (PDX) tumor was harvested, and dissociated tumor cells were printed as a mixed bioprint. The mixed bioprinted tumor was minced and implanted into the flank of athymic nude mice and allowed to grow until it reached the Institutional Animal Care and Use Committee parameters before harvesting for histology and immunohistochemistry. (D) The histology of the COA109 bioprinted microtumor (left panel) implanted into the flank was similar to the human PDX tumor grown in the murine flank (Figure 1E, middle panel). The COA109 bioprinted flank tumor stained positive for chromogranin A (right panel),consistent with a neuroendocrine tumor. Negative control staining with immunoglobulin (Ig)G was performed for each run of immunostaining and is represented by the insets in at the lower right corner of the photomicrographs.

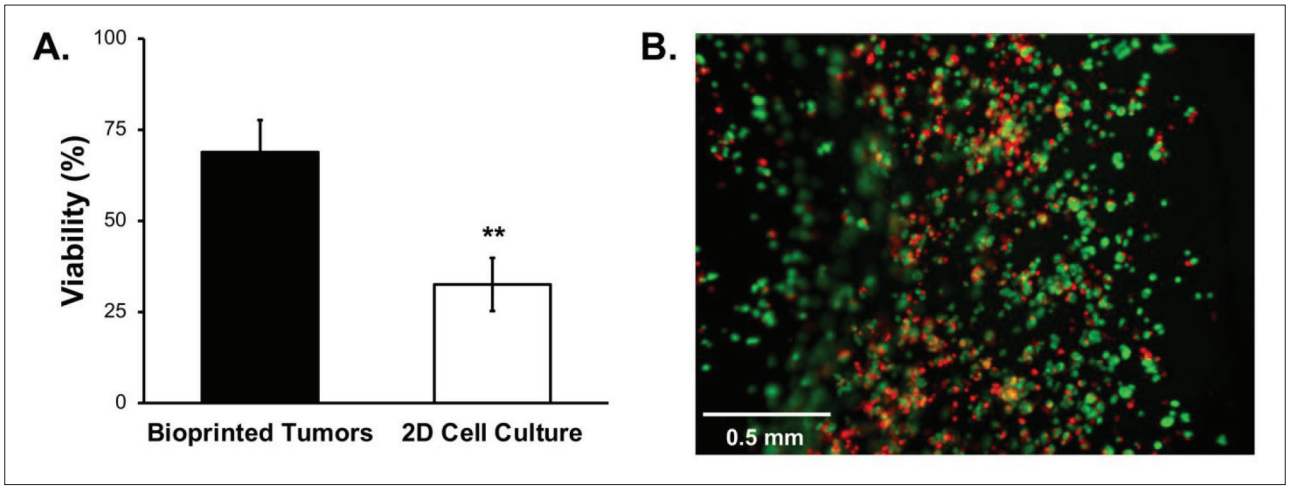

Figure 3. Bioprinted tumors are resistant to hypoxia.SK-N-AS cells were printed in a layered method (5×10^5 cells per print) or in 2D culture (5×10^4 cells per well) in 12-well plates and incubated under 1% oxygen. After 5 days, the bioprinted tumors and 2D-cultured cells were stained with Calcein AM and alamarBlue, respectively, to assess viability. (A) The percentage of viable cells in the SK-N-AS bioprints was significantly greater (69%) than that of viable SK-N-AS cells grown in 2D culture (33%). (B) A representative fluorescence microscopy of the bioprint showing dead tumor cells (red) surrounded by viable tumor cells (green). Data represent at least three biologic replicates and were reported as mean ± standard error of the mean (SEM) and evaluated with two-tailed t-test. $^{**}P \leq 0.01$.

3.5. Optimization of bioprinted models for high-throughput studies

In order to render the bioprinted tumors more conducive to high-throughput studies, the methods used to produce mixed bioprinted models were scaled down to 96-well plates (Figure 5A). We repeated the experiments previously described in Figure 4 in 96-well plates and compared the bioprinted tumors to cells plated in 2D culture. Bioprinted tumors and 2D-cultured cells were treated for 24 h with increasing drug concentrations. With this model, we were able to use a more rapid colorimetric assay to detect changes in viability. Compared to cells grown in 2D culture, COA6 bioprinted tumors were less sensitive to cisplatin (Figure 5B). Similar findings were noted with SK-N-AS bioprinted tumors, which were less sensitive to cisplatin than SK-N-AS cells in 2D culture (Figure 5C), and PDX COA109 bioprinted tumors, which were less sensitive to trametinib than COA109 cells in 2D culture (Figure 5D).

4. Discussion

The translation of targeted molecular therapies for pediatric cancers from the bench to human clinical trials has remained a stagnant process, averaging six and a half years longer for pediatric versus adult cancers[20]. The delay is partially due to the smaller patient population[1]. Other barriers to developing better pediatric cancer drugs include suboptimal preclinical models that poorly replicate human conditions and the complex heterogeneity of pediatric solid tumors[21]. Therefore, we aimed to create a 3D bioprinting model that could provide a more accurate depiction of treatment response.

In order to improve cancer outcomes, treatments have focused on targeted molecular therapies based on tumor mutations or genetic aberrations. For example, a pancreatic cancer study has demonstrated that nearly one-third of treatment regimens were altered based on tumor genomic sequence[22]. Achieving this personalized approach based on genomics entails a multistep process, which includes tumor biopsy, tumor genetic sequencing, and drug panel screening. Excluding drug panel tests, reports have suggested that the median duration to identify a personalized therapeutic in adult malignancies is 60 days[23]. Given that the median time to relapse or disease progression in high-risk neuroblastoma patients is 14 months and may occur as early as 1 month in some instances[24], a timeline of 60 days to design applicable interventions is unrealistic. Additionally, in a study by Cobain *et al.*, who investigated the success of targeted therapies based on genetic sequencing, only 37.1% received clinical benefit[25], thus calling into question the advantage of genomic testing before drug panel screening. In order to expedite the process, we envision a model where the patient's cancer cells are bioprinted and undergo high-throughput testing with a drug panel to identify the best therapeutic intervention (**Supplementary File**, **Figure S3**). As an ongoing area of research for our lab, we have yet to directly print cells from patients. However, in the current study, we focused on demonstrating the feasibility of bioprinting pediatric tumors that recapitulate the tumor

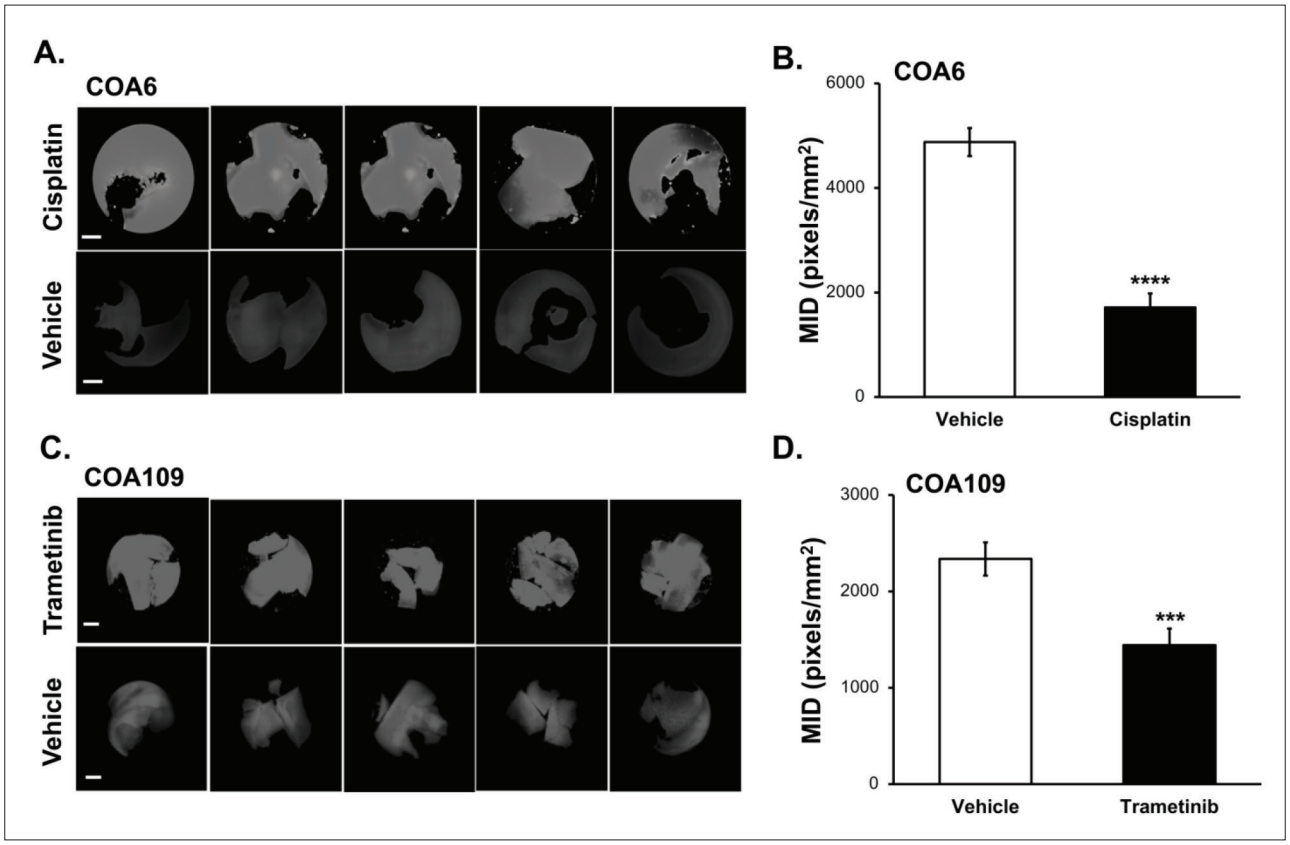

Figure 4. Bioprinted models for *ex vivo* testing of therapeutics. (A) COA6 (10^7 cells per print) mixed bioprinted tumors were treated with 10 μM cisplatin (n=5) or vehicle (n=5) for 10 days and stained with Calcein AM to assess viability. Images of the bioprinted tumors were taken using Cytation 5 and converted into 8-bit grayscale images for analysis of viability in ImageJ. (B) Viability of the COA6 bioprinted tumors treated with cisplatin demonstrated a lower mean integrated density (MID) (1713 ± 306 pixels/mm^2) than those treated with vehicle (4878 ± 268 pixels/mm^2). (C) A similar study was conducted with COA109 (10^7 cells per print) mixed bioprinted tumors. The COA109 bioprinted tumors were treated with 100 nM of trametinib for 10 days. Viability was measured in the same fashion as in (A). (D) COA109 bioprinted tumors treated with trametinib had a lower MID (1442 ± 120 pixels/mm^2) than those treated with vehicle (2336 ± 172 pixels/mm^2). Photomicrographs represent individual bioprinted tumors. Data represent at least five bioprinted tumors andwere reported as mean ± standard error of the mean (SEM) and evaluated with Student's t-test. Scale bars represent 1 mm. ***$P \leq 0.001$, ****$P \leq 0.0001$.

phenotype and that could be employed for testing of potential therapeutics in an *ex vivo* fashion.

2D cell culture lacks the physical properties that render solid tumors challenging to treat, making 2D culture suboptimal when compared to 3D culture options[26]. For example, in 2D culture, nearly all cells are equally exposed to the agent under investigation, whereas *in vivo*, the cells located exteriorly, near the vasculature, may experience a higher exposure to the agent compared to cells located within the tumor core[27]. In the current study, there was a higher percentage of nonviable tumor cells located on the periphery of the bioprinted tumors following treatment, which may be demonstrative of this phenomenon. The same logic applies to nutrient supply. *In vivo*, tumors exist in a hypoxic and nutrient-depleted environment, which may lead to a more aggressive phenotype[28,29]. In 2D culture, all cells experience a relatively abundant and equal amount of O_2, glucose, and other nutrients. We predict that the cells in the core of the 3D-bioprinted tumor may experience hypoxia and nutrient deprivation, rendering them more similar to human tumor conditions. In the hypoxia experiment presented here, we found less tumor cell death in the bioprinted tumors when subjected to hypoxia. Other than that, the structure of tumors also gives rise to spatial heterogeneity. For instance, in a murine model of glioblastoma, different regions of tumor harbored distinct mutations[30]. This heterogeneity has also been demonstrated by Braekeveldt *et al.* in neuroblastoma PDXs and further corroborated in avatar PDX models of neuroblastoma[31]. Single-cell sequencing on 16 neuroblastoma patients has shown 160 different signatures that may contribute to malignancy in neural crest cells. Within a neuroblastoma tumor, cells harbor different copy number variants, and these subclones may prove central to tumor progression[32]. This variability renders single, targeted, therapeutic interventions challenging

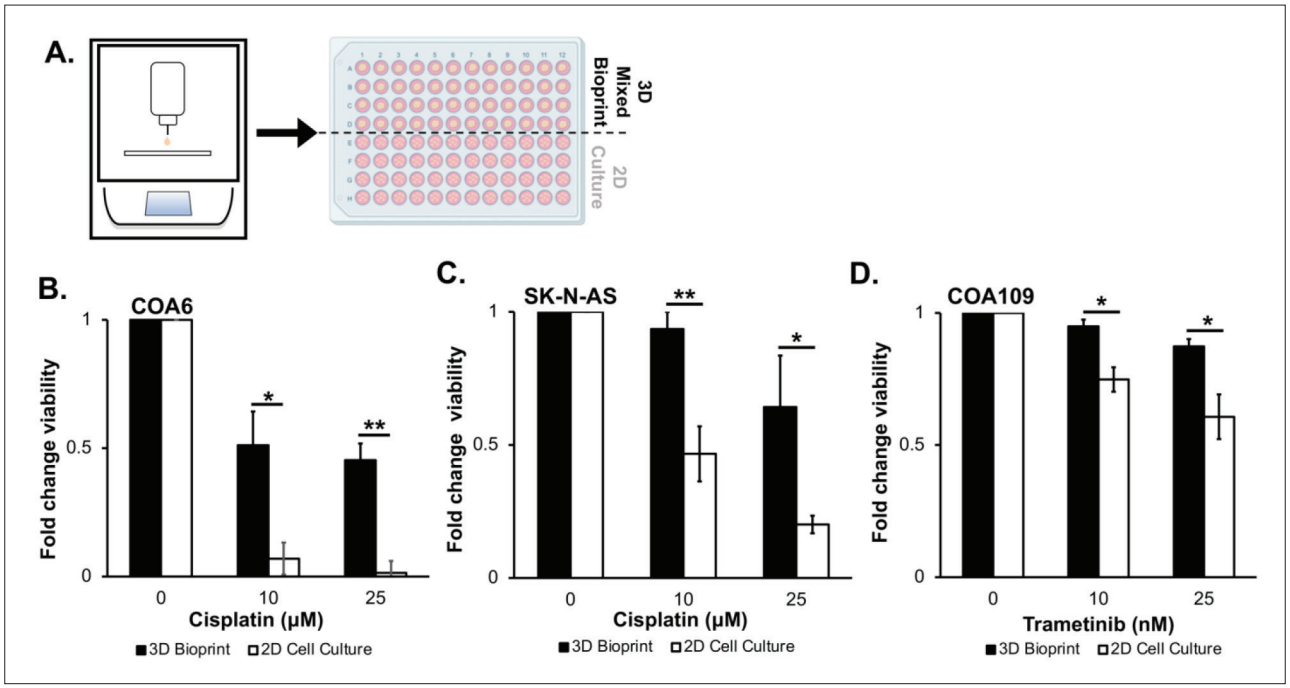

Figure 5. High-throughput drug testing using bioprinted models. (A) Using Cellink'sthree-dimensional (3D) printer, cancer cells were mixed with 1 mL of bioink to produce bioprinted tumors on a 96-well plate (upper rows). The bioprinted tumors were printed on the same plate as cells in traditional 2D cell culture for direct comparison (lower rows). (B) Human neuroblastoma patient-derived xenograft (PDX) COA6 cells (10^7) and (C) established neuroblastoma cell line SK-N-AS cells (10^7) were printed. The bioprinted tumors were treated with cisplatin at increasing concentrations (0–25 μM) for 24 h, and their viability was assessed with alamarBlue and compared with cells plated (1.5×10^4) and treated with cisplatin (0–25 μM) for 24 h in 2D culture. The 3D-bioprinted COA6 (B) and SK-N-AS (C) tumors were less sensitive to cisplatin than cells grown in 2D culture conditions. (D) COA109 human neuroendocrine PDX cells (10^7) were printed as mixed tumors in 96-well plates. The bioprinted tumors were treated with trametinib at increasing concentrations (0–25 nM) for 24 h, and their viability was also assessed with alamarBlue and compared with COA109 cells plated (1.5×10^4) and treated with trametinib (0–25 nM) in 2D culture for 24 h. Compared to 2D-cultured cells, the 3D-bioprinted tumors were less sensitive to trametinib treatment. Data represent three biologic replicates andwere reported as mean ± standard error of the mean (SEM) and evaluated with Student's t-test. *$P \leq 0.05$, **$P \leq 0.01$.

and explains the diverse clinical response often seen with conventional therapies[25,33]. Future directions would involve examining the spatial transcriptomics of the bioprinted models.

The use of 3D bioprinting as a research tool in pediatric cancers is uncommon. In the few previous reports, researchers have primarily utilized osteosarcoma, glioblastoma, and neuroblastoma[13,34,35]. In neuroblastoma, bioprinting studies were not focused on its use as cancer models but rather on the potential to generate artificial neural networks and the ability of tumor cells to differentiate into viable, differentiated neural cells in sodium alginate gel[36-39]. These researchers have raised concerns that their findings may indicate that PDXs and established cell lines would undergo differentiation and lose their cancer properties in the bioink[37]. To the best of our knowledge, the current study is novel in its demonstration that the cells do not differentiate and the bioprinted models clearly recapitulate the solid tumor phenotype of PDX neural crest tumors. Pediatric solid tumors are hallmarked by their heterogeneity. We believe that creating models that closely represent human conditions for study will require the inclusion of heterogeneous cell populations. The use of cancer stem cells (CSCs) to create spheroids, as 3D tumor models, has been reported[6]. We did not limit our model to CSCs as these cells comprise only a small portion of the tumor and would differentiate into non-stem tumor cells after undergoing self-renewal[40].

The bioprinted SK-N-AS, COA6, and COA109 cell lines retained the histology and staining characteristics of the original tumors. Furthermore, the bioprinted tumors grew after being implanted into mice. Other bioprinted models of neuroblastoma have focused on tumor vasculature, where models with patent channels surrounding a body of tumor cells have been developed. In those studies, the ability to perform drug testing or demonstrate tumor phenotypes has not been reported[41,42]. The bioprint designs in the current study did not have any preconstructed channels to mimic vessels; instead, the bioink, as a porous substance, allowed the penetration of therapeutic agents into the

bioprint, as demonstrated in the experiments employing cisplatin and trametinib treatments in the bioprints, and tumor growth *in vivo*, which requires nutrient diffusion and capillary in growth.

Ning *et al.* recently published the results of a photo-crosslinked model of a vascularized bioprinted neuroblastoma and included human embryonic endothelial cells (HUVECs) into the print to demonstrate the role of endothelial cells in neuroblastoma tumor biology[42]. Compared to 2D culture and prints without HUVECs, neuroblastoma bioprints with HUVECs had significantly more tumor cells that infiltrated and traveled further into the gel matrix; additionally, bioprints with HUVECs had the highest glucose uptake, suggesting that they are more metabolically active. HUVECs have demonstrated the ability to use ultraviolet (UV) light to crosslink bioprinted neuroblastoma tumors and alter the stiffness of the bioprint matrix by adjusting UV exposure times. For our prints, we relied on calcium chloride and adjusted the volume as well as duration to obtain the optimal stiffness for each print. Although calcium chloride may be a harsher method for crosslinking, it does not introduce nonlethal DNA damage, which may result from using UV light for crosslinking. We noted minimal loss of viability with chemical crosslinking but intend to investigate the use of photo-crosslinking with non-UV rays for future studies.

Here, we used conventional therapeutics and demonstrated that the bioprinted models were more resistant to therapies than cells in conventional 2D culture. Similar findings have been observed in other studies. Grunewald *et al.* used bioprints to test the chimeric antigen receptor (CAR) T-cell therapy; using a gelatin and hyaluronic bioink, they produced 3D-bioprinted tumors of SK-N-BE(2) human neuroblastoma cells and demonstrated less CART-cell-induced cytolysis of neuroblastoma cells in the bioprint than in 2D culture[43]. Their findings and those of the current study highlight the discrepancy in treatment efficacy observed when transitioning therapies from the bench to the bedside and suggest that bioprinted models could provide better preclinical insights into the potential success of a therapy.

An advantage of 3D-bioprinted tumors is the opportunity to explore the contributions of the TME. In neural crest-derived solid tumors, the TME may contribute to their poor response to therapy. In neuroblastoma, for example, there are significantly less activated $CD8^+$ cells in the TME as a result of *MYCN*-transcribed immunosuppressive signals, which may partially explain the disappointing results realized thus far with CART-cell therapy for these tumors[44]. The ability to incorporate tumor heterogeneity and TME into models for preclinical drug testing is crucial for developing and evaluating new therapies for pediatric neural crest-derived tumors that will successfully translate to clinical use. Researchers have demonstrated the ability to incorporate immune cells into the bioprints of breast and pancreatic cancers as they would be in a tumor *in vivo*[8]. In neuroblastoma, HUVECs and fibroblasts have been added to 3D bioprints to better recapitulate the TME[42]. We did not include non-tumor cells into the bioprinted models in the current study. The next iteration of the model for refinement will involve creating 3D-bioprinted models with cellular components of the TME.

5. Conclusion

In this study, we demonstrated that a 3D bioprinter used in conjunction with a sodium alginate and gelatin bioink could be utilized to design bioprinted neural crest-derived tumors that mimic their original tumor phenotypes, including cell morphology, resistance to hypoxia, and chemotherapeutic resistance. Concurrently, we also scaled the process to a format that is amenable to high-throughput screening. We envision this technology to be useful in preclinical settings for investigating potential cancer treatments for both global treatments and individualized therapeutics.

Acknowledgments

We wish to thank Dr. David Crossman, Dr. Mike Crowley, and the UAB Genomics Core for their assistance in validating the PDXs.

Funding

This project was made possible by funding from the National Cancer Institute of the National Institutes of Health under award numbers 5T32GM008361: Medical Scientist Training Program (CHQ), T32 CA229102 (LVB), and P30 CA013148 to the Genomics Core at the University of Alabama at Birmingham. The content is solely the responsibility of the authors and does not necessarily represent the official views of the National Institutes of Health. Other funding sources include Sid Strong Foundation, Elaine Roberts Foundation, Open Hands Overflowing Hearts, Starr Fund-Vince Lombardi Cancer Foundation, and Hyundai Hope on Wheels (EAB). Funding for portions of the study included NIH/NCI U01 CA223976 and U01 CA223976-03S1 (CDW).

Conflict of interest

The authors declare no conflict of interests.

Author contributions

Conceptualization: Colin H. Quinn, Andee M. Beierle, Christopher D. Willey, Elizabeth A. Beierle

Data acquisition: Colin H. Quinn, Andee M. Beierle, Janet R. Julson, Michael E. Erwin, Hasan Alrefai, Hooper R. Markert, Sara Claire Hutchins, Laura V. Bownes

Formal analysis: Colin H. Quinn, Michael E. Erwin, Hooper R. Markert, Elizabeth Mroczek-Musulman

Funding acquisition: Christopher D. Willey, Elizabeth A. Beierle

Investigation: Colin H. Quinn, Andee M. Beierle, Janet R. Julson, Michael E. Erwin, Hasan Alrefai, Hooper R. Markert, Sara Claire Hutchins, Laura V. Bownes

Resources: Jerry E. Stewart, Jamie M. Aye, Patricia H. Hicks, Karina J. Yoon, Christopher D. Willey, Elizabeth A. Beierle

Supervision: Elizabeth A. Beierle

Writing – original draft: Colin H. Quinn, Andee M. Beierle, Elizabeth A. Beierle

Writing – review & editing: Colin H. Quinn, Andee M. Beierle, Elizabeth A. Beierle

Ethics approval and consent to participate

Tumors were obtained as previously described under the University of Alabama at Birmingham (UAB) Institutional Review Board (IRB)-approved protocol (IRB 130627006) and in accordance with the Declaration of Helsinki as well as the guidelines of the National Institutes of Health. Informed consent was obtained from all guardians and assent from patients where appropriate prior to study enrollment.

Consent for publication

Informed consent was obtained from all guardians and assent from patients where appropriate to publish their data in this study.

Availability of data

The data from these studies are available from the corresponding author, Dr. Elizabeth A. Beierle, upon reasonable request.

References

1. Siegel RL, Miller KD, Fuchs HE, *et al.*, 2022, Cancer statistics. *CA Cancer J Clin,* 72(1):7–33.

   https://doi.org/10.3322/caac.21708

2. Colon NC, Chung DH, 2011, Neuroblastoma. *Adv Pediatr,* 58(1):297–311.

   https://doi.org/10.1016/j.yapd.2011.03.011

3. Navalkele P, O'Dorisio MS, O'Dorisio TM, *et al.*, 2011, Incidence, survival, and prevalence of neuroendocrine tumors versus neuroblastoma in children and young adults: Nine standard SEER registries, 1975-2006. *Pediatr Blood Cancer,* 56(1):50–57.

   https://doi.org/10.1002/pbc.22559

4. LeSavage BL, Suhar RA, Broguiere N, *et al.*, 2022, Next-generation cancer organoids. *Nat Mater,* 21(2):143–159.

   https://doi.org/10.1038/s41563-021-01057-5

5. Kang Y, Datta P, Shanmughapriya S, *et al.*, 2020, 3D bioprinting of tumor models for cancer research. *ACS Appl Bio Mater,* 3(9):5552–5573.

   https://doi.org/10.1021/acsabm.0c00791

6. Zhuang P, Chiang YH, Fernanda MS, *et al.*, 2021, Using spheroids as building blocks towards 3D bioprinting of tumor microenvironment. *Int J Bioprint,* 7(4):444.

   https://doi.org/10.18063/ijb.v7i4.444

7. Neufeld L, Yeini E, Reisman N, *et al.*, 2021, Microengineered perfusable 3D-bioprinted glioblastoma model for in vivo mimicry of tumor microenvironment. *Sci Adv,* 7(34):eabi9119.

   https://doi.org/10.1126/sciadv.abi9119

8. Langer EM, Allen-Petersen BL, King SM, *et al.*, 2019, Modeling tumor phenotypes in vitro with three-dimensional bioprinting. *Cell Rep,* 26(3): 608–623 e6.

   https://doi.org/10.1016/j.celrep.2018.12.090

9. Stafman LL, Williams AP, Marayati R, *et al.*, 2019, Focal adhesion kinase inhibition contributes to tumor cell survival and motility in neuroblastoma patient-derived xenografts. *Sci Rep,* 9(1):13259.

   https://doi.org/10.1038/s41598-019-49853-z

10. Quinn CH, Beierle AM, Williams AP, *et al.*, 2021, Downregulation of PDGFRss signaling overcomes crizotinib resistance in a TYRO3 and ALK mutated neuroendocrine-like tumor. *Transl Oncol,* 14(7):101099.

    https://doi.org/10.1016/j.tranon.2021.101099

11. Marayati R, Bownes LV, Quinn CH, *et al.*, 2021, Novel second-generation rexinoid induces growth arrest and reduces cancer cell stemness in human neuroblastoma patient-derived xenografts. *J Pediatr Surg,* 56(6):1165–1173.

    https://doi.org/10.1016/j.jpedsurg.2021.02.041

12. Stafman LL, Mruthyunjayappa S, Waters AM, *et al.*, 2018, Targeting PIM kinase as a therapeutic strategy in human hepatoblastoma. *Oncotarget,* 9(32):22665–22679.

    https://doi.org/10.18632/oncotarget.25205

13. Quinn CH, Beierle AM, Hutchins SC, *et al.*, 2022, Targeting high-risk neuroblastoma patient-derived xenografts with oncolytic virotherapy. *Cancers (Basel),* 14(3):762.

    https://doi.org/10.3390/cancers14030762

14. Tomayko MM, Reynolds CP, 1989, Determination of subcutaneous tumor size in athymic (nude) mice. *Cancer Chemother Pharmacol,* 24(3):148–154.

    https://doi.org/10.1007/BF00300234

15. Hirabayashi K, Zamboni G, Nishi T, *et al.*, 2013 Histopathology of gastrointestinal neuroendocrine neoplasms. *Front Oncol,* 3:2.

    https://doi.org/10.3389/fonc.2013.00002

16. Bownes LV, Williams AP, Marayati R, *et al.*, 2021, Serine-threonine kinase receptor-associated protein (STRAP) knockout decreases the malignant phenotype in neuroblastoma cell lines. *Cancers (Basel),* 13(13):3201.

    https://doi.org/10.3390/cancers13133201

17. Hockel M,Vaupel P, 2001, Biological consequences of tumor hypoxia. *Semin Oncol,* 28(2 Suppl 8):36–41.

    https://www.ncbi.nlm.nih.gov/pubmed/11395851.

18. Jogi A, Ora I, Nilsson H, *et al.*, 2002, Hypoxia alters gene expression in human neuroblastoma cells toward an immature and neural crest-like phenotype. *Proc Natl Acad Sci U S A,* 99(10):7021–7026.

    https://doi.org/10.1073/pnas.102660199

19. Braekeveldt N, Bexell D, 2018, Patient-derived xenografts as preclinical neuroblastoma models. *Cell Tissue Res,* 372(2):233–243.

    https://doi.org/10.1007/s00441-017-2687-8

20. Neel DV, Shulman DS, DuBois SG, 2019, Timing of first-in-child trials of FDA-approved oncology drugs. *Eur J Cancer,* 112:49–56.

    https://doi.org/10.1016/j.ejca.2019.02.011

21. Byron SA, Hendricks WPD, Nagulapally AB, *et al.*, 2021, Genomic and transcriptomic analysis of relapsed and refractory childhood solid tumors reveals a diverse molecular landscape and mechanisms of immune evasion. *Cancer Res,* 81(23):5818–5832.

    https://doi.org/10.1158/0008-5472.CAN-21-1033

22. Aguirre AJ, Nowak JA, Camarda ND, *et al.*, 2018, Real-time genomic characterization of advanced pancreatic cancer to enable precision medicine.*Cancer Discov,* 8(9):1096–1111.

    https://doi.org/10.1158/2159-8290.CD-18-0275

23. Reda M, Richard C, Bertaut A, *et al.*, 2020, Implementation and use of whole exome sequencing for metastatic solid cancer. *EBioMedicine,* 51:102624.

    https://doi.org/10.1016/j.ebiom.2019.102624

24. Murphy JM, Lim IIP, Farber BA, *et al.*, 2016, Salvage rates after progression of high-risk neuroblastoma with a soft tissue mass. *J Pediatr Surg,* 51(2):285–288.

    https://doi.org/10.1016/j.jpedsurg.2015.10.075

25. Cobain EF, Wu YM, Vats P, *et al.*, 2021, Assessment of clinical benefit of integrative genomic profiling in advanced solid tumors.*JAMA Oncol,* 7(4):525–533.

    https://doi.org/10.1001/jamaoncol.2020.7987

26. Kapalczynska M, Kolenda T, Przybyla W, *et al.*, 2018, 2D and 3D cell cultures—A comparison of different types of cancer cell cultures. *Arch Med Sci,* 14(4):910–919.

    https://doi.org/10.5114/aoms.2016.63743

27. Stylianopoulos T, Jain RK, 2013, Combining two strategies to improve perfusion and drug delivery in solid tumors. *Proc Natl Acad Sci U S A,* 110(46):18632–18637.

    https://doi.org/10.1073/pnas.1318415110

28. Brown JM, Wilson WR, 2004, Exploiting tumour hypoxia in cancer treatment. *Nat Rev Cancer*, 4(6):437–447.

    https://doi.org/10.1038/nrc1367

29. Bhandari V, Hoey C, Liu LY, *et al.*, 2019, Molecular landmarks of tumor hypoxia across cancer types. *Nat Genet*, 51(2):308–318.

    https://doi.org/10.1038/s41588-018-0318-2

30. Li Y, Li B, Li W, *et al.*, 2020, Murine models of IDH-wild-type glioblastoma exhibit spatial segregation of tumor initiation and manifestation during evolution. *Nat Commun,* 11(1):3669.

    https://doi.org/10.1038/s41467-020-17382-3

31. Braekeveldt N, von Stedingk K, Fransson S, *et al.*, 2018, Patient-derived xenograft models reveal intratumor heterogeneity and temporal stability in neuroblastoma. *Cancer Res,* 78(20):5958–5969.

    https://doi.org/10.1158/0008-5472.CAN-18-0527

32. Dong R, Yang R, Zhan Y, *et al.*, 2020, Single-cell characterization of malignant phenotypes and developmental trajectories of adrenal neuroblastoma. *Cancer Cell,* 38(5):716–733.e6.

    https://doi.org/10.1016/j.ccell.2020.08.014

33. Manas A, Aaltonen K, Andersson N, *et al.*, 2022, Clinically relevant treatment of PDX models reveals patterns of neuroblastoma chemoresistance.*Sci Adv,* 8(43):eabq4617.

    https://doi.org/10.1126/sciadv.abq4617

34. Pellegrini E, Desando G, Petretta M, *et al.*, 2022, A 3D collagen-based bioprinted model to study osteosarcoma invasiveness and drug response. *Polymers (Basel),* 14(19):4070.

    https://doi.org/10.3390/polym14194070

35. Tang M, Xie Q, Gimple RC, *et al.*, 2020, Three-dimensional bioprinted glioblastoma microenvironments model cellular dependencies and immune interactions. *Cell Res,* 30(10):833–853.

    https://doi.org/10.1038/s41422-020-0338-1

36. Chen Q, Tian X, Fan J, *et al.*, An interpenetrating alginate/gelatin network for three-dimensional (3D) cell cultures and organ bioprinting.*Molecules,* 25(3):756.

https://doi.org/10.3390/molecules25030756

37. Bordoni M, Karabulut E, Kuzmenko V, *et al.*, 3D printed conductive nanocellulose scaffolds for the differentiation of human neuroblastoma cells. *Cells,* 9(3):682.

https://doi.org/10.3390/cells9030682.

38. Fantini V, Bordoni M, Scocozza F, *et al.*, 2019 Bioink composition and printing parameters for 3D modeling neural tissue. *Cells,* 8(8):830.

https://doi.org/10.3390/cells8080830

39. Jury M, Matthiesen I, Boroojeni FR, *et al.*, 2022, Bioorthogonally cross-linked hyaluronan-laminin hydrogels for 3D neuronal cell culture and biofabrication. *Adv Healthc Mater,* 11(11):e2102097.

https://doi.org/10.1002/adhm.202102097

40. Bao B, Ahmad A, Azmi AS, *et al.*, 2013, Overview of cancer stem cells (CSCs) and mechanisms of their regulation: Implications for cancer therapy. *Curr Protoc Pharmacol,* Chapter 14:Unit 14 25.

https://doi.org/10.1002/0471141755.ph1425s61

41. Nothdurfter D, Ploner C, Coraca-Huber DC, *et al.*, 2022, 3D bioprinted, vascularized neuroblastoma tumor environment in fluidic chip devices for precision medicine drug testing. *Biofabrication,*14(3).

https://doi.org/10.1088/1758-5090/ac5fb7

42. Ning L, Shim J, Tomov ML, *et al.*, 2022, A 3D bioprinted in vitro model of neuroblastoma recapitulates dynamic tumor-endothelial cell interactions contributing to solid tumor aggressive behavior. *Adv Sci (Weinh),* 9(23):e2200244,

https://doi.org/10.1002/advs.202200244

43. Grunewald L, Lam T, Andersch L, *et al.*, 2021, A reproducible bioprinted 3D tumor model serves as a preselection tool for CAR T cell therapy optimization. *Front Immunol,* 12:689697.

https://doi.org/10.3389/fimmu.2021.689697

44. Wu X, Nelson M, Basu M, *et al.*, 2021, MYC oncogene is associated with suppression of tumor immunity and targeting Myc induces tumor cell immunogenicity for therapeutic whole cell vaccination. *J Immunother Cancer,* 9(3):e001388.

https://doi.org/10.1136/jitc-2020-001388